Full Azimuth Seismic Modeling in the Norwegian Sea

Marianne Houbiers[1], Børge Arntsen[1], Joachim Mispel[1], Edward Hager[2], Gordon Brown[2], and David Hill[2]*
1) StatoilHydro Research Center, Trondheim, Norway
2) WesternGeco, Schlumberger House, Buckingham Gate, Gatwick Airport, RH6 0NZ, UK

SUMMARY

One of the fields in the Norwegian Sea has been imaged several times over the past decades, both with conventional narrow azimuth seismic surveys as well as with ocean bottom seismic. The extensively faulted structure of the field and the possible presence of a salt diapir cause imaging problems in some areas. Therefore, a simulation study has been initiated to judge whether or not a marine full azimuth acquisition geometry improves the image of the subsurface.

For this simulation study, simplified velocity and density models of the field were created, containing the main features characterizing it, as well as the problem areas. The simulation was done with 3D finite difference (FD) modeling. Data sets with and without free surface multiples were generated, and imaging from a full azimuth acquisition geometry was compared with imaging from a conventional narrow azimuth geometry.

FD modeling shows that the full azimuth design generally leads to a better suppression of noise in the data, mainly due to increased fold. Depth slices show that fault edges are imaged sharper in a full azimuth geometry. Also, the image of and below the salt/limestone structure is improved. However, attenuation of multiple energy due to increased cross line fold is less than expected, except for the first seabed multiple. The low maximum frequency used in FD-modeling may have limited the increase in image quality with the full azimuth modeling.

INTRODUCTION

The field of interest in this study is located in the Norwegian Sea, west of the coast of Mid-Norway. The geological strata below the Base Cretaceous Unconformity (BCU) are intensely faulted and the reservoir of the field is segmented into many compartments. The field was put on stream in the mid-nineties, but a few parts are still not fully understood because of imaging problems. In particular, a dome shaped feature in what is called the M-segment, causes a very disturbed image. Earlier, it was assumed that the dome is caused by a salt diapir sourced by Triassic salt. A recent study shows that there are some high impedance limestone banks of seep deposits located around the dome. In addition, in some specific areas of the field, faults and dip directions are unclear, giving rise to dipping conflicts below the BCU. In spite of several vintages of seismic data, it has not been possible to obtain a much clearer seismic image of these problem areas, although multiples caused by the strong impedance variations around the dome seem to be attenuated better in ocean bottom seismic (OBS) data.

For a good seismic image of a subsurface point, a proper illumination is needed. That means, one needs an adequate distribution of offsets and azimuths, or in other words, a look from all directions. Conventional survey geometries tend to look in one direction only, i.e., sources and receivers are placed along a line with a uniform distribution of offset values. In a marine full azimuth (FAZ) geometry, the objective is not only to vary the offset, but also the azimuth. A FAZ geometry intends to copy the offset azimuth distribution of an OBS survey, but with usual streamer vessels and thus against lower costs. Regone (2006) shows that a wide azimuth design leads to a better suppression of noise in the data – in particular multiples – and as a consequence, one obtains better images, especially in a complex subsurface and below salt structures. However, this result was obtained in the Gulf of Mexico, which has a very different geological structure and is about three times deeper as the reservoir considered in this study.

Earlier, an illumination study of the top and the bottom of the reservoir of the field has been performed. Based on ray tracing results, there was not found any indication for acquisition-related anomalies for the two target horizons, nor was there found a significant difference in the illumination for two orthogonal shooting directions. This could be interpreted as an indication that a FAZ design would not give a better image. However, the model used in this illumination study might not be detailed enough to see small local differences, especially since ray tracing has practical problems with strongly faulted areas. In addition, FD-modeling gives more accurate estimates of seismic amplitudes on horizons than ray tracing, and the effect of multiples and multiple suppression can be studied better. Therefore it is very useful to do a FAZ-modeling study. This paper describes some of the results of the simulation study.

The paper is organized as follows. First, the velocity and density models of the field that are used for modeling are described. Second, the modeling geometries and corresponding CPU-requirements are discussed. Subsequently, modeling results for a conventional narrow azimuth (NAZ) survey are compared with a FAZ survey, both for the case with and without multiples. The paper ends with some concluding remarks.

Full Azimuth Modeling in the Norwegian Sea

VELOCITY MODEL

The velocity and density models that are constructed for the simulation study preserve the main features characterizing the field, as well as the problem areas. The structural model coincides with the original inline and crossline system, that is, the cell size is 12.5 meter in local x and y coordinates. The same grid size is used in the z-direction. The model extends over 10875 m in local x-direction and 19475 m in local y-direction, and has a total depth of 3800 m. The local coordinate system is rotated 23.42 degrees clockwise from North.

The structural model contains a overburden with weak lateral variation, a faulted reservoir section, and a section below the reservoir. The overburden contains five horizons, and the reservoir section contains six horizons, including the top and the base of the reservoir. The base of the reservoir is a coal marker. Below the reservoir, an additional coal marker is included. There are roughly speaking two main fault systems at the field, crossing each other at an angle of about 45° (one system runs about north-south, the other one southwest-northeast). Nine main faults and two internal faults are included in the reservoir section of the model. The two internal faults are representing ‘problem-faults’ in two areas with unclear faults and dipping conflicts. Except for two faults which have a lower average dip, the faults included in the model have an average dip of 40 to 60°. Finally, at the dome shaped feature in the M-segment, two limestone discs and a small salt body are included.

The horizons in the structural model form layers, and within the reservoir, these layers are subdivided into fault blocks. The regions corresponding to the layers, fault blocks, coal markers, limestone discs and salt body, are filled with velocities and densities. P-velocities in each layer are obtained from depth migration velocities in that layer. The depth migration velocities have a gradient in the z-direction: $V(x,y,z) = V_0(x,y) + kz$. However, not all horizons included in the present model have a corresponding ‘constant’ $V_0(x,y)$-grid and gradient k in the depth migration velocity grid. Neither are faults present. To create impedance contrasts at these extra horizons and at the fault planes, well data has been used. Roughly speaking, a constant value has been added in each layer/fault block, such that the p-velocity at the wells in that layer/fault block on average is the same as the average from the logs. The density for the model is obtained from Gardner’s power law velocity-density relationship $\rho(x,y,z) = d \cdot (V(x,y,z)/1000)^f$ (Gardner et al., 1974), where the prefactor d and the exponent f are detemined in an earlier study and are set to $d = 1568.9$ and $f = 0.3669$, respectively. The p-velocities and densities in special areas such as the salt body are given in the table below.

Feature	P-velocity (m/s)	Density (kg/m^3)
Water	1480	1002
Upper limestone disc	4700	2400
Lower limestone disc	4700	2500
Salt body	4500	2200
Coal markers	2400	1500

Table 1. Overview of p-velocities and densities at special areas in model.

The velocity and density of the coal markers, which both have a thickness of 25 meter, are obtained from visual inspection of the well logs. The two coal markers are relatively strong reflectors, giving rise to internal multiples. Cross sections of the model are displayed in Figs 1a, 2a, and 3a.

FD MODELING

For the FD-modeling, the model was extended with 7 km in x- and y-direction. Acoustic modeling was done with 3D FD-modeling (Holberg, 1987). The modeling was done on a cluster with 128 nodes with 4 cpu’s each, and 8Gb of memory per cpu. To reduce computation time and memory usage, the model was resampled from 12.5 to 25m in each direction. With the extension mentioned above, the size of the model is 996 x 1340 x 153 grid cells.

A displacement source with a Ricker wavelet was used. Given the water velocity of 1480 m/s and gridding of 25 m, a maximum frequency of 23 Hz was used for the displacement source, with a delay of 0.2s. The actual maximum frequency for the pressure waves is slightly higher as the second derivative of the displacement source occurs in the wave equation.

Modeling is done using a super geometry with 320 x 320 receivers on a 25 x 25 m grid, i.e., a 8 x 8km receiver grid. The source is put in the middle of the receiver grid. The local aperture used in the modeling is a 10 x 10 x 3.8 km cube. The shot distance is 50 m in the local x-direction, and sail lines are separated by 500 m in the y-direction. The first shot is located at x = 1 km and y = 5 km in local coordinates. Each sail line contains 201 shots. With 25 sail lines, the total number of shots is 5025. With an FD-time step of 1 ms and a recording length of 5 seconds, and given the size of the aperture, each shot takes about 1 day on one cpu. During modeling, 420 shots are processed in parallel, such that it takes about 12 days to model 5025 shots. Pressure is recorded every 8 ms. Modeling is done both with and without free surface multiples.

The source was put at a depth of 25 m, the receivers at 50 m. In the modeling, an operator half length of 8 was used in time and space dimensions. PML boundary conditions are used, with a 15 node boundary zone in all directions. When modeling with multiples, there is no boundary zone at the sea surface.

From the super geometry, a conventional streamer geometry is obtained by selecting a receiver configuration with 10 streamers separated by 100 m, and a cable length of 3850 m with the first receiver 150 m behind the source. Receiver distance is 25 m, shot distance is 50 m and sail lines are separated by 500 m, as in the full geometry. The full geometry has an inline fold of 80 and a cross line fold of 8, whereas the conventional geometry has inline fold of 38, and a cross line fold of 1.

The data are migrated with shot-profile finite difference depth migration, with the same velocity model as the one used in modeling. Before migration, the direct wave is subtracted from the shot gathers and the time delay is removed. No other preprocessing was done. Migration is done with an 10 x 10 km aperture for the full data set, and 10 x 5 km aperture for the receiver subset representing the conventional geometry. The source is again located in the middle of the aperture. In both cases, migration is done to a depth of 3.8 km. Frequencies between 4 and 28 Hz are migrated. Migration takes about 2 hours per shot on one cpu for the full data set, and half the time for the conventional geometry.

RESULTS

Figures 1 to 3 display the results of the modeling and migration. In Figure 1, a cross line through the salt diapir and limestone discs is shown. Figure 2 shows an inline in the northern part, and Figure 3 shows a depth slice at 2625 m. The dashed lines in each figure show the position of the cross sections in the other figures. Each figure shows the velocity model (A), the migrated data for the FAZ geometry without (B) and with free surface multiples (C), and the conventional NAZ geometry with multiples (D). Migrated data for the conventional NAZ geometry without multiples are not displayed here, but they confirm the results described below.

The spatial resolution of the vertical sections in Figures 1 and 2 are limited due to the low maximum frequency used for modeling. In addition, source and receiver ghosts from the sea surface increase the spatial extend of the wavelet, and decrease the spatial resolution further (the receiver ghost also has a notch at 15 Hz). As a consequence, many details visible in the velocity model are not visible in the migrated image, in particular in the case with free surface multiples.

At a first glance, there seems to be little difference between the full azimuth and conventional design. The conventional geometry is slightly more noisy, as is most clearly visible on the depth slices in Figure 3. This is expected as the fold of the full geometry is on average a factor 16 higher, increasing the signal to noise ratio.

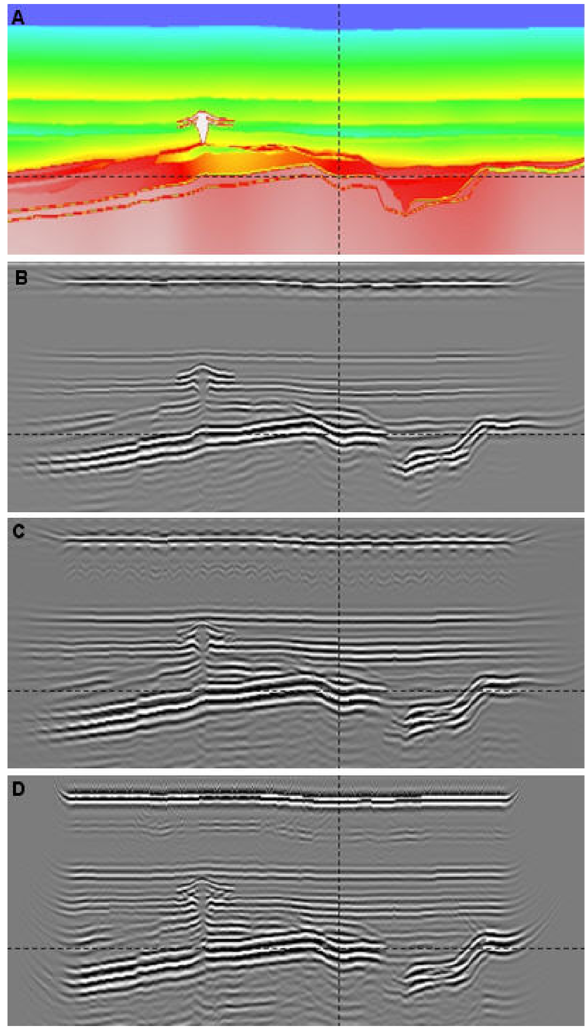

Figure 1: Cross line through salt diapir and limestone discs. A) velocity model, B) FAZ imaging without multiples, C) FAZ imaging with multiples, and D) NAZ imaging with multiples.

The full geometry gives a better illumination of and below the limestone/salt structure, see Figure 1. The flanks and the bottom of the salt diapir, and the horizons below it are better imaged in the full geometry, compared to the conventional geometry. Also, the fault planes are imaged slightly sharper and with less artifacts in the full geometry, as is best visible on depth slices, see Figure 3. On the vertical slices in Figures 1 and 2, the fault planes are not so clear due to the low resolution.

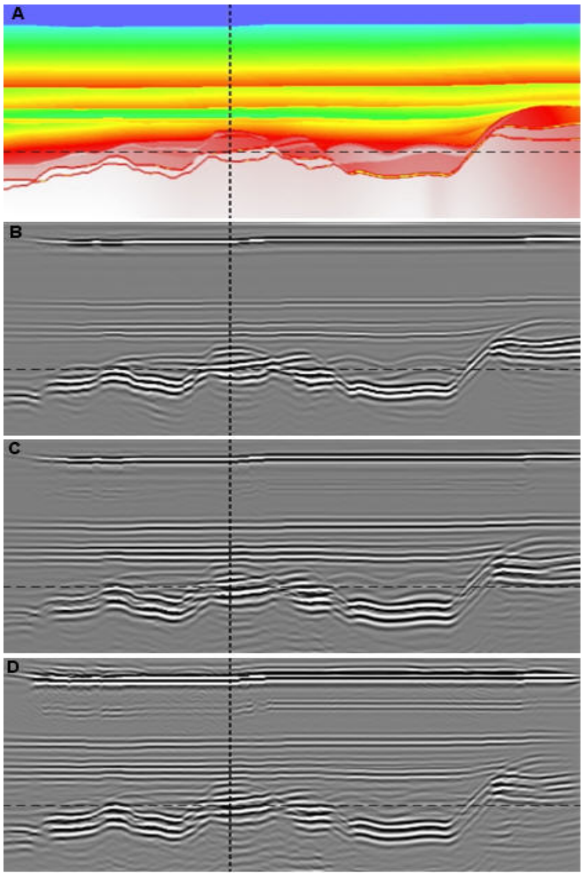

Figure 2: Cross section through model along inline. A) Velocity model B) FAZ imaging without multiples C) FAZ imaging with multiples, and D) NAZ imaging with multiples.

One of the ideas behind increased crossline offset and fold is that multiples in the data are better attenuated. Indeed, the first seabed multiple is attenuated better in the FAZ geometry, see Figures 1 and 2. Notice that whereas the seafloor and its first multiple in the conventional geometry are visible as more or less continuous horizons along the crossline displayed in Figure 1, they are rather rugged in the FAZ geometry. This is the fingerprint of the acquisition geometry with sparse sampling in the crossline direction compared to the inline direction.

There are also other multiples visible. For instance, the image of the horizons in the graben on the right hand side in Figure 2 seems more distorted by multiples in the conventional NAZ geometry. In the FAZ geometry, these multiples are slightly better suppressed. But in general, the attenuation of multiples in the FAZ geometry is less than expected. In particular, attenuation of multiples due to the coal markers is only marginally improved. A study using one-way wave equation modeling confirms this result. This is rather surprising, as one of the ideas behind a full azimuth survey is to reduce multiple energy.

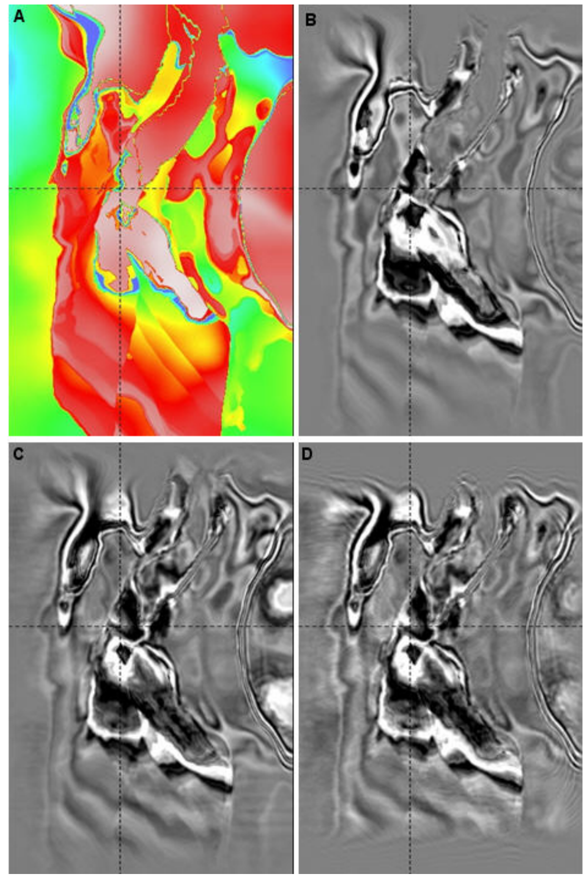

Figure 3: Depth slice through model at 2625 m. A) Velocity model B) FAZ imaging without multiples C) FAZ imaging with multiples, and D) NAZ imaging with multiples.

CONCLUSION

A finite difference modeling study shows that a full azimuth survey improves the seismic image of a small salt diapir and the horizons below. Also, fault planes are imaged sharper due to increased fold. However, attenuation of multiple energy with increased crossline offset and fold is less than expected. This is not anticipated to be different in a realistic survey design.

The results obtained are influenced by the limited maximum frequency (resolution) used in the modeling, and the limited amount of preprocessing. Moreover, differences between a full azimuth and the conventional geometry might become more pronounced when the velocity model is estimated from the data. Illumination maps on particular horizons may also reveal local differences in amplitudes.

EDITED REFERENCES

Note: This reference list is a copy-edited version of the reference list submitted by the author. Reference lists for the 2008 SEG Technical Program Expanded Abstracts have been copy edited so that references provided with the online metadata for each paper will achieve a high degree of linking to cited sources that appear on the Web.

REFERENCES

Gardner, G. H. F., L. W. Gardner, and A. R. Gregory, 1974, Formation velocity and density: The diagnostic basics for stratigraphic traps: Geophysics, **39**, 770–780.

Holberg, O., 1987, Computational aspects of the choice of operator and sampling interval for numerical differentiation in large-scale simulation of wave phenomena: Geophysical Prospecting, **35**, 629–655.

Regone, C. J., 2006, A modeling approach to wide-azimuth design for subsalt imaging: The Leading Edge, **25**, 1467–1475.